Synthesis and Structure of Strontium and Barium Guanidinates and Mixed-Ligand Guanidinate Pentamethylcyclopentadienyl Complexes

Thomas M. Cameron,*,† Chongying Xu,† Antonio G. Dipasquale,‡ and Arnold L. Rheingold‡

ATMI Inc., 7 Commerce Drive, Danbury, Connecticut 06810, and Department of Chemistry and Biochemistry, University of California, San Diego, La Jolla, California 92093-0358

Received November 5, 2007

A new family of strontium and barium guanidinate complexes were synthesized from SrI_2, $[Sr\{N(SiMe_3)_2\}_2]_2$, $[Ba\{N(SiMe_3)_2\}_2(THF)_{1.6}]$, $Sr(Cp^*)_2$, and $Ba(Cp^*)_2(THF)_{1.7}$ metal reactants and appropriate guanidine or guanidinate ligand (Cp^* = pentamethylcyclopentadienide). Treatment of $[Sr\{N(SiMe_3)_2\}_2]_2$ with 4.0 equiv of *i*PrN═C(NMe$_2$)N(H)*i*Pr (**1**LH) or *i*PrN═C(N(*i*Pr)$_2$)N(H)*i*Pr (**2**LH) gave dimeric complexes $[(\eta^2\text{-}\mathbf{1}L)Sr(\mu^2,\eta^2{:}\eta^2\text{-}\mathbf{1}L)(\mu^2,\eta^1{:}\eta^1\text{-}\mathbf{1}L)Sr(\eta^2\text{-}\mathbf{1}L)]$ (**3**) and $[(\eta^2\text{-}\mathbf{2}L)Sr(\mu^2,\eta^2{:}\eta^2\text{-}\mathbf{2}L)_2Sr(\eta^2\text{-}\mathbf{2}L)]$ (**4**), respectively. Related reactions of **1**LH and **2**LH with 1.0 equiv of $Sr(Cp^*)_2$ afforded the mixed-ligand complexes $[(Cp^*)Sr(\mu^2,\eta^2{:}\eta^2\text{-}\mathbf{1}L)_2Sr(Cp^*)]$ (**5**) and $[(Cp^*)Sr(\mu^2,\eta^2{:}\eta^2\text{-}\mathbf{2}L)_2Sr(Cp^*)]$ (**6**), respectively, with simultaneous liberation of Cp*H. Treatment of $[Ba\{N(SiMe_3)_2\}_2(THF)_{1.6}]$ with 2.0 equiv of **2**LH gave the dimer $[(\eta^2\text{-}\mathbf{2}L)Ba(\mu^2,\eta^2{:}\eta^2\text{-}\mathbf{2}L)_2Ba(\eta^2\text{-}\mathbf{2}L)]$ (**7**), while reaction of $Ba(Cp^*)_2(THF)_{1.7}$ with **2**LH afforded guanidinate-bridged $[(Cp^*)Ba(\mu^2,\eta^2{:}\eta^2\text{-}\mathbf{2}L)_2Ba(Cp^*)]$ (**8**). Reaction of SrI_2 with 2.0 equiv of Na[(*i*Pr)NC(N(SiMe$_3$)$_2$)N(*i*Pr)] (**9**LNa) in diethyl ether gave monomeric $[Sr(\eta^2\text{-}\mathbf{9}L)_2OEt_2]$ (**10**). The solid-state structures of **3**, **4**, **6**, **7**, **8**, and **10** are reported. Reactions of **4** and **6** with certain Lewis bases are also described.

Introduction

Interest in the organometallic chemistry of the heavier alkaline earth elements, strontium and barium, has been driven by their potential application in organic synthesis,[1] anionic styrene polymerization,[2] and thin films for solid-state devices.[3] New compound discovery in this area is often hampered by poor compound stability and the propensity for forming oligomeric, poorly soluble, and poorly volatile species, a result of the large ionic radius and low charge density of the strontium and barium metal centers. These problems have been largely overcome by synthetic approaches using sterically demanding hydrocarbyl,[2,4] β-diketiminate,[5] indene,[6] and cyclopentadienyl ligands[7] to promote encapsulation of the metal center, resulting in stable, soluble, monomeric compounds. In an effort to discover novel, structurally interesting, well-defined, heavy alkaline earth complexes, we exploited the steric and electronic tunability of the guanidine/guanidinate ligand to access guanidinate complexes.[8] Here we present our initial findings in this area and report on the synthesis and structure of new strontium and barium guanidinates and mixed-ligand pentamethylcyclopentadienyl (Cp*)-guanidinate complexes generated via a facile transamination route. We also detail the interaction of the reported compounds with Lewis bases. The mixed-ligand Cp*-guanidinate complexes are rare examples of structurally characterized, non-halide-containing,[9] mixed Cp* compounds. To our knowledge the only known, crystallographically characterized, related strontium or barium mixed-ligand Cp compounds are the

* Corresponding author. E-mail: tcameron@atmi.com.
† ATMI Inc.
‡ University of California, San Diego.

(1) Yanagisawa, A.; Habaue, S.; Yasue, K.; Yamamoto, H. *J. Chem. Soc., Chem. Commun.* **1996**, 367.

(2) (a) Weeber, A.; Harder, S.; Brintzinger, H. H. *Organometallics* **2000**, *19*, 1325. (b) Feil, F.; Harder, S. *Eur. J. Inorg. Chem.* **2003**, 3401. (c) Feil, F.; Harder, S. *Eur. J. Inorg. Chem.* **2005**, 4438. Reports of calcium-mediated anionic styrene polymerization have also appeared. (d) Harder, S.; Feil, F.; Weeber, A. *Organometallics* **2001**, *20*, 1044. (e) Harder, S.; Feil, F.; Knoll, K. *Angew. Chem., Int. Ed.* **2001**, *40*, 4261. (f) Harder, S.; Feil, F. *Organometallics* **2002**, *21*, 2268. (g) Feil, F.; Müller, C.; Harder, S. *J. Organomet. Chem.* **2003**, *683*, 56.

(3) (a) Hatanpää, T.; Vehkamäki, M.; Mutikainen, I.; Kansikas, J.; Ritala, M.; Leskelä, M. *Dalton. Trans.* **2004**, 1181. (b) Ihanus, J.; Hänninen, T.; Hatanpää, T.; Aaltonen, T.; Mutikainen, I.; Sajavaara, T.; Keinonen, J.; Ritala, M.; Leskelä, M. *Chem. Mater.* **2004**, *14*, 1937. (c) Vehkamäki, M.; Hänninen, T.; Ritala, M.; Leskelä, M.; Sajavaara, T.; Rauhala, E.; Keinonen, J. *Chem. Vap. Deposition* **2001**, *7*, 75. (d) Vehkamäki, M.; Hatanpää, T.; Hänninen, T.; Ritala, M.; Leskelä, M. *Electrochem. Solid-State Lett.* **1999**, *2*, 504.

(4) (a) Cloke, F. G. N.; Hitchcock, P. B.; Lappert, M. F.; Lawless, G. A.; Royo, B. *J. Chem. Soc., Chem. Commun.* **1991**, 724. (b) Green, D. C.; Englich, U.; Ruhlandt-Senge, K. *Angew. Chem., Int. Ed.* **1999**, *38*, 354.

(5) (a) Clegg, W.; Coles, S. J.; Cope, E. K.; Mair, F. S. *Angew. Chem., Int. Ed.* **1998**, *37*, 796. (b) El–Kaderi, H. M.; Heeg, M. J.; Winter, C. H. *Organometallics* **2004**, *23*, 4995. (c) Harder, S. *Organometallics* **2002**, *21*, 3782.

(6) Overby, J. S.; Hanusa, T. P. *Organometallics* **1996**, *15*, 2205.

(7) (a) For reviews see: Hanusa, T. P. *Chem. Rev.* **1993**, *93*, 1023. (b) Hanusa, T. P. *Organometallics* **2002**, *21*, 2559. (c) For specific $C_5Me_5(Cp^*)$ examples see: Burns, C. J.; Andersen, R. A. *J. Organomet. Chem.* **1987**, *325*, 31. (d) Williams, R. A.; Hanusa, T. P.; Huffmann, J. C. *Organometallics* **1990**, *9*, 1128. (e) For $C_5H_2(CHMe_2)_3$ see: Burkey, D. J.; Williams, R. A.; Hanusa, T. P. *Organometallics* **1993**, *12*, 1331. (f) For $C_5H(CHMe_2)_4$ see: Williams, R. A.; Tesh, K. F.; Hanusa, T. P. *J. Am. Chem. Soc.* **1991**, *113*, 4843. (g) For $C_5(CHMe_2)_5$ see: Sitzmann, H.; Dezember, T.; Ruck, M. *Angew. Chem., Int. Ed. Engl.* **1998**, *37*, 3114. (h) For $C_5H_2(SiMe_3)_3$ see: Harvey, M. J.; Quisenberry, K. T.; Hanusa, T. P.; Young, V. G. *Eur. J. Inorg. Chem.* **2003**, 3383. (i) For $C_5H_2(CMe_3)_3$ see: Weber, F.; Sitzmann, H.; Schultz, M.; Sofield, C. D.; Andersen, R. A. *Organometallics* **2002**, *21*, 3139.

(8) One example of a strontium guanidinate has appeared in the literature; see ref 2c.

(9) (a) Sitzmann, H.; Weber, F.; Walter, M. D.; Wolmershäuser, G. *Organometallics* **2003**, *22*, 1931. (b) Harvey, M. J.; Hanusa, T. P. *Organometallics* **2000**, *19*, 1556.

10.1021/om701118j CCC: $40.75
Publication on Web 03/08/2008

Scheme 1[a]

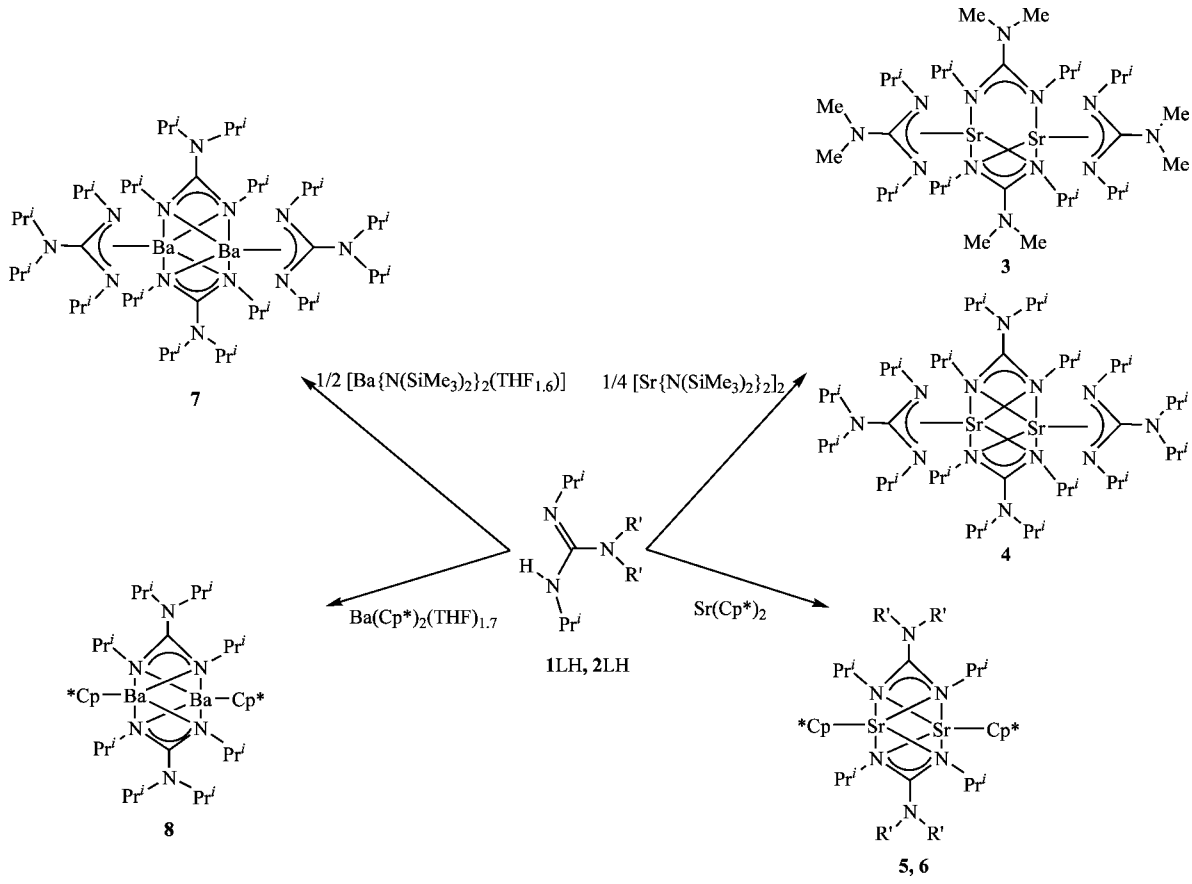

[a] **1**: R′ = Me; **2**: R′ = *i*Pr; **5**: R′ = Me; **6**: R′ = *i*Pr.

recently described triple-decker cyclooctatetraenyl (COT) complexes[10] and an enolate-bridged strontium complex.[11]

Results and Discussion

By taking advantage of a straightforward trans-amination route, we were able to generate strontium and barium guanidinate species. Reaction of metal amide precursor $[Sr\{N(SiMe_3)_2\}_2]_2$ with 4.0 equiv of the guanidine bases *i*PrN=C(NMe$_2$)N(H)*i*Pr (**1**LH) or *i*PrN=C(N(*i*Pr)$_2$)N(H)*i*Pr (**2**LH) at 20 °C gave the dimeric and homoleptic complexes [(η^2-**1**L)Sr(μ^2,η^2:η^2-**1**L)(μ^2,η^1:η^1-**1**L)Sr(η^2-**1**L)] (**3**) and [(η^2-**2**L)Sr(μ^2,η^2:η^2-**2**L)$_2$Sr(η^2-**2**L)] (**4**), respectively (Scheme 1). Compounds **3** and **4** crystallize from the reaction mixture overnight and can be isolated by filtration in 69% and 72% yield, respectively. Complexes **3** and **4** were characterized by single-crystal X-ray studies. The thermal ellipsoid plots of **3** and **4** are shown in Figures 1 and 2, respectively, and the details of the structure refinement appear in Table 1. In the solid-state structure of **3**, the guanidinate ligands have three different bonding modes, η^2-terminal, μ^2,η^2:η^2-bridging, and μ^2,η^1:η^1-bridging, that support each metal center in a distorted five-coordinate geometry. The bite angles of the η^2-terminal guanidinate ligands N(4)−Sr(2)−N(5) and N(1)−Sr(1)−N(2) of 53.57(6)° and 52.88(6)°, respectively, are slightly less acute than the bite angles associated with the μ^2,η^2:η^2-bridging ligand of N(10)−Sr(2)−N(11) 49.94(5)° and N(10)−Sr(1)−N(11) 48.70(5)°. The acute ligand bite angles in **3** make the distinction between five-coordinate trigonal bipyramidal or square-pyramidal geometry difficult at first sight. An analysis of **3** according to the criteria proposed by Reedijk *et al*. gives τ = 0.27 for Sr(2), where τ describes the geometry about each metal center as between the two extremes, where τ = 0 for square-pyramidal and τ = 1 for trigonal-bipyramidal coordination modes.[12] The presence of three distinct guanidinate bonding modes in **3** allows for a direct bonding mode vs bond length comparison. The η^2-terminal guanidinate bond lengths of Sr(1)−N(1) 2.5296(19) Å, Sr(1)−N(2) 2.5577(18) Å, Sr(2)−N(4) 2.5549(17) Å, and Sr(2)−N(5) 2.5067(17) Å are characteristic of an η^2-terminal strontium−guanidinate interaction and are similar to the average Sr−N bond length of 2.524(3) Å reported for [Sr{(Cy)NC(N(SiMe$_3$)$_2$)N(Cy)}$_2$·(Et$_2$O)], a related complex with two η^2-terminal strontium−guanidinate interactions,[2c] and to 2.583(9) Å (average) for Sr−N bonds in amidinate complex [PhC(NSiMe$_3$)$_2$]$_2$Sr(THF)$_2$.[13] The μ^2,η^1:η^1-bridging guanidinate−metal interaction in **3** is characterized by Sr(1)−N(7) and Sr(2)−N(8) distances of 2.4982(19) and 2.5501(18) Å, respectively. The similar N(7)−C(19) and N(8)−C(19) bond lengths of 1.330(3) and 1.336(3) Å, respectively, support delocalization of the formal monoanionic charge equally through the N(7)−C(19)−N(8) unit. It is not surprising then that the metal−nitrogen contacts for η^2-terminal and μ^2,η^1:η^1-bridging

(10) Walter, M. D.; Wolmershäuser, G.; Sitzmann, H. *J. Am. Chem. Soc.* **2005**, *127*, 17494.
(11) Westerhausen, M.; Hartmann, M.; Makropoulos, N.; Wieneke, B.; Wieneke, M.; Schwarz, W.; Stalke, D. *Z. Naturforsch.* **1998**, *53B*, 117.
(12) Addison, A. W.; Rao, T. N.; Reedijk, J.; van Rijin, J.; Verschoor, G. C. *J. Chem. Soc., Dalton Trans.* **1984**, 1349.
(13) Westerhausen, M.; Hausen, H. D.; Schwarz, W. *Z. Anorg. Allg. Chem.* **1992**, *618*, 121.

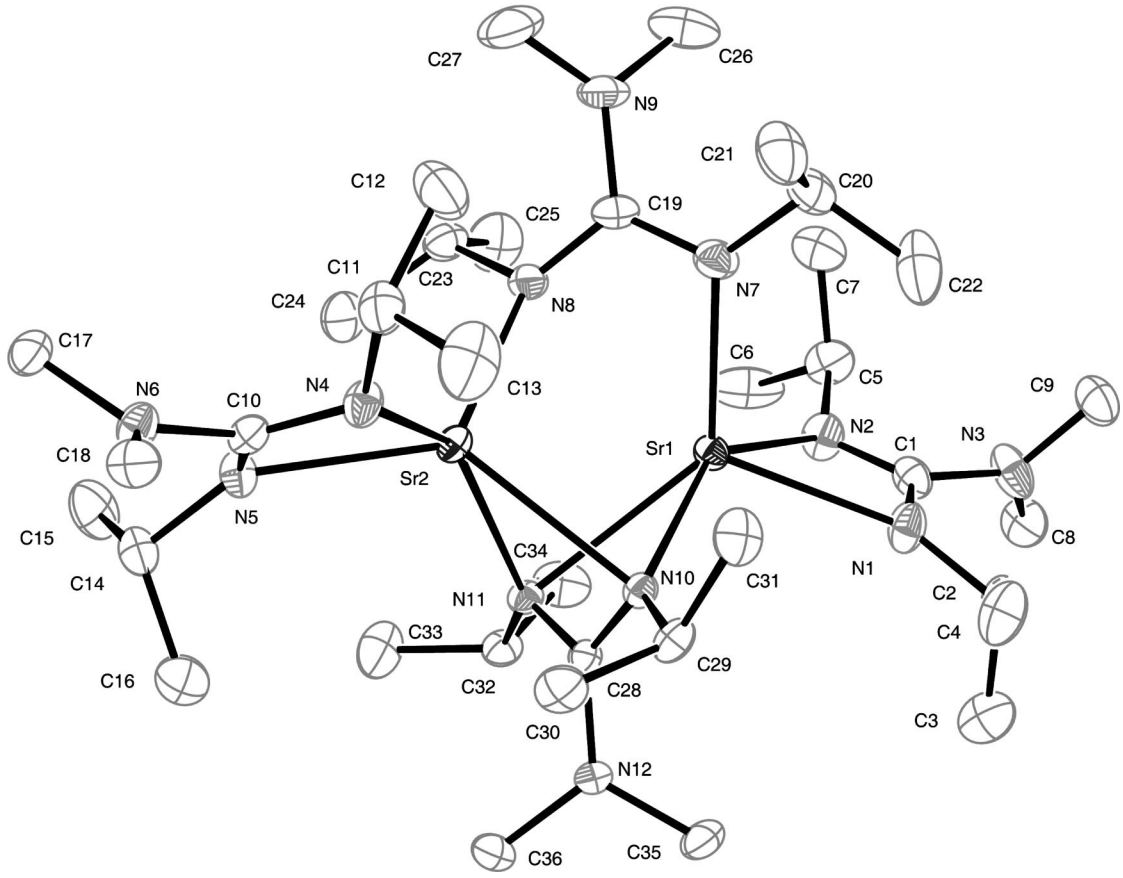

Figure 1. Thermal ellipsoid plot of **3** (30% probability thermal ellipsoids). Selected bond lengths (Å) and angles (deg): Sr(1)–N(7) 2.4982(19), Sr(1)–N(10) 2.6713(15), Sr(1)–N(11) 2.7902(16), Sr(1)–N(1) 2.5296(19), Sr(1)–N(2) 2.5577(18), Sr(2)–N(10) 2.6730(16), Sr(2)–N(11) 2.6678(16), Sr(2)–N(8) 2.5501(18), Sr(2)–N(4) 2.5549(17), Sr(2)–N(5) 2.5067(17), N(7)–C(19) 1.330(3), N(8)–C(19) 1.336(3), Sr(1)–Sr(2) 3.5728(3), N(4)–C(10)–N(5) 118.12(18), N(7)–C(19)–N(8) 117.79(19), N(2)–C(1)–N(1) 117.7(2), N(10)–C(28)–N(11) 114.83(17), N(1)–Sr(1)–N(2) 52.88(6), N(4)–Sr(2)–N(5) 53.57(6), N(10)–Sr(1)–N(11) 48.70(5), N(10)–Sr(2)–N(11) 49.94(5).

modes fall within the same range, as each nitrogen atom interacts with only one metal center. In contrast, N(10) and N(11) of the $\mu^2,\eta^2:\eta^2$-bridging ligand each interact with both metal centers, Sr(1) and Sr(2), and should have the longest metal−nitrogen distances in **3**. The Sr(1)−N(10) and Sr(2)−N(10) distances of 2.6713(15) and 2.6730(16) Å and the Sr(1)−N(11) and Sr(2)−N(11) distances of 2.7902(16) and 2.6678(16) Å, respectively, are longer than those associated with η^2-terminal and $\mu^2,\eta^1:\eta^1$-bridging bonding modes, as expected. The Sr−N distances of 2.9860(18) Å for Sr(1)−N(8) and 3.763 Å for Sr(2)−N(7) are both longer than the sum of the ionic radius of Sr^{2+} and the van der Waals radius of nitrogen (2.87 Å) and for that reason are not being considered as significant metal−nitrogen interactions.[14] For comparative purposes, values of 2.435(2) Å (terminal) and 2.638(4) Å (bridging) have been reported for Sr−N single bond interactions in dimeric $[Sr\{N(SiMe_3)_2\}_2]_2$.[15]

The ^{1}H NMR spectrum of **3** at 60 °C contains two doublet resonances at 1.24 and 1.40 ppm assigned to *i*Pr methyl groups and two singlets at 2.77 and 3.65 ppm assigned to guanidinate NCH_3 methyl groups.[16] There are therefore only two different guanidinate environments present on the NMR time scale at 60 °C and not three, as the solid-state structure would suggest. A rapid exchange between the two guanidinate bridging modes, on the NMR time scale, at this temperature could account for this observation. A variable-temperature ^{1}H NMR spectroscopy experiment was undertaken on a sample of **3** dissolved in d_8-toluene. The ^{1}H NMR spectrum of **3** remained unchanged to −83 °C, suggesting that any fluxional processes are still fast on the NMR time scale at −83 °C.

In contrast to the solid-state structure of **3**, there are only two guanidinate bonding modes in **4**, η^2-terminal and $\mu^2,\eta^2:\eta^2$-bridging, resulting in six-coordinate metal centers (Figure 2). The η^2-terminal-ligand-to-metal contacts of 2.562(2), 2.568(2), 2.566(2), and 2.567(2) Å are all shorter than each $\mu^2,\eta^2:\eta^2$-bridging-ligand-to-metal contact, where the average $\mu^2,\eta^2:\eta^2$-bridging-ligand-to-metal bond distance is 2.736(2) Å. As observed in **3**, the bite angles of the η^2-terminal guanidinate ligands are all less acute than the bite angles associated with the $\mu^2,\eta^2:\eta^2$-bridging ligands, consistent with the longer metal to $\mu^2,\eta^2:\eta^2$-bridging ligand distance. The Sr(1)−Sr(2) distance of 3.4455(5) Å in **4** is substantially shorter than the Sr(1)−Sr(2) distance of 3.5728(3) Å in **3**. The $\mu^2,\eta^1:\eta^1$-bridging mode present in **3** increases the nonbonding Sr−Sr distance with respect to the distance in **4**.

The solution-state structure of **4** is consistent with the results of the single-crystal X-ray study. Analysis of the ^{1}H NMR spectrum of **4** at 60 °C in C_6D_6 reveals the presence of four doublets at 1.20, 1.23, 1.30, and 1.48 ppm corresponding to the methyl groups from four inequivalent *i*Pr environments.[16]

(14) Radius for Sr^{2+} (coordination number 6), van der Waals radius for nitrogen, and radius for Ba^{2+} (coordination number 6) taken from: Huheey, J. E. *Inorganic Chemistry*, 3rd ed.; Harper & Row: New York, 1983.

(15) Westerhausen, M.; Schwarz, W. Z. *Anorg. Allg. Chem.* **1991**, *606*, 177.

(16) The elevated temperature of 60 °C was used during the NMR experiment to completely solubilize the compound. The NMR spectrum of a sample at 20 °C was unchanged from that at 60 °C.

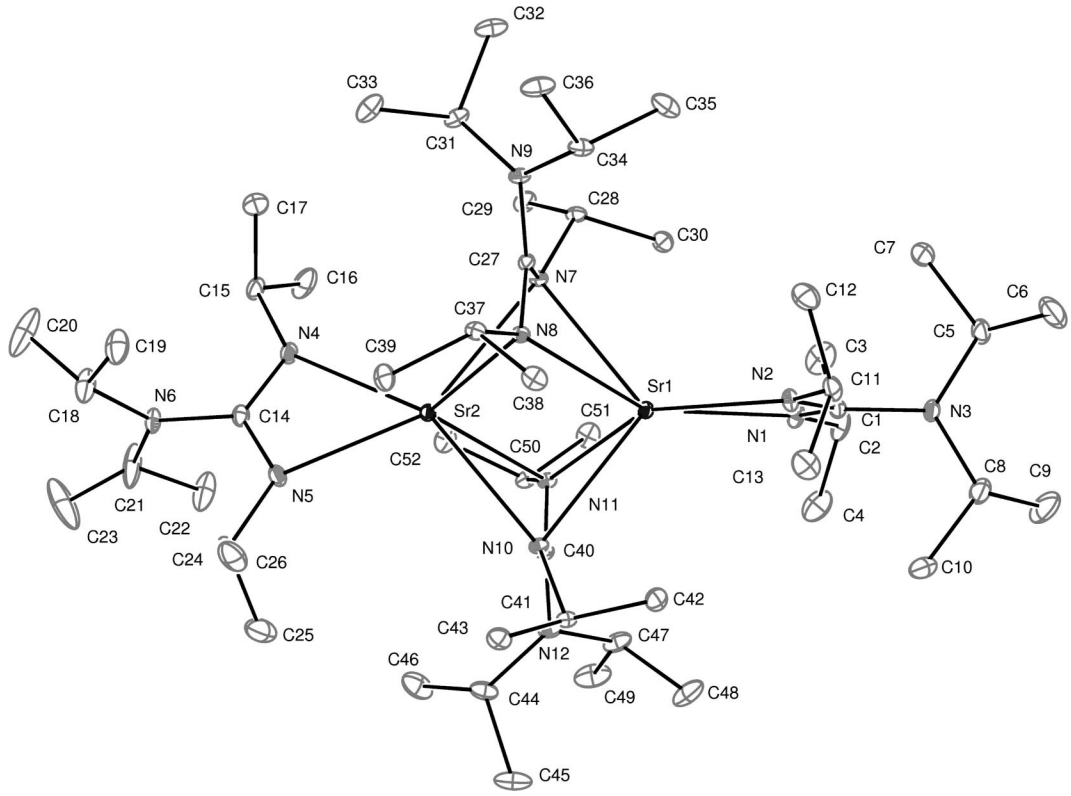

Figure 2. Thermal ellipsoid plot of **4** (30% probability thermal ellipsoids). Selected bond lengths (Å) and angles (deg): Sr(1)–N(1) 2.562(2), Sr(1)–N(2) 2.568(2), Sr(1)–N(7) 2.709(2), Sr(1)–N(8) 2.762(2), Sr(1)–N(10) 2.709(2), Sr(1)–N(11) 2.765(2), Sr(2)–N(4) 2.566(2), Sr(2)–N(5) 2.567(2), Sr(2)–N(7) 2.747(2), Sr(2)–N(8) 2.721(2), Sr(2)–N(10) 2.754(2), Sr(2)–N(11) 2.719(2), Sr(1)–Sr(2) 3.4455(5), N(1)–C(1)–N(2) 117.3(2), N(7)–C(27)–N(8) 114.3(2), N(10)–C(40)–N(11) 114.8(2), N(4)–C(14)–N(5) 116.8(2), N(1)–Sr(1)–N(2) 52.56(8), N(4)–Sr(2)–N(5) 52.38(8), N(7)–Sr(1)–N(8) 48.66(6), N(10)–Sr(1)–N(11) 48.57(6), N(7)–Sr(2)–N(8) 48.70(6), N(10)–Sr(2)–N(11) 48.60(6).

Table 1. Summary of Crystallographic Data and Structure Refinement Details for 3, 4, and 6

	3	**4**	**6**
empirical formula	$C_{36}H_{80}N_{12}Sr_2$	$C_{52}H_{112}N_{12}Sr_2$	$C_{46}H_{86}N_6Sr_2$
fw	856.36	1080.78	898.45
space group	$P\bar{1}$	*Pbca*	$P2_1/n$
a (Å)	9.8910(6)	15.2890(18)	12.0150(15)
b (Å)	11.8040(7)	23.481(3)	12.6800(16)
c (Å)	21.6540(13)	34.845(4)	16.614(2)
α (deg)	90.6080(10)	90	90
β (deg)	93.6150(10)		102.513(2)
γ (deg)	111.0420(10)		
V_c (Å^3)	2353.4(2)	12 509(3)	2471.0(5)
D_c (Mg m^{-3})	1.208	1.148	1.208
Z	2	8	2
μ(Mo Kα) (mm^{-1})	2.303	1.746	2.193
final *R* indices[a]	R1 = 0.0330 wR2 = 0.0801 [10 611]	R1 = 0.0438 wR2 = 0.0932 [14 962]	R1 = 0.0362 wR2 = 0.0806 [5832]

[a] $R1 = \sum F_o| - |F_c/\sigma|F_o|$ and $wR2 = [\sum[w(F_o^2 - F_c^2)^2]/\sum[w(F_o^2)^2]]^{1/2}$. The parameter $w = 1/[\sigma^2(F_o^2) + (aP)^2]$.

Each guanidinate ligand has two inequivalent *i*Pr groups, and there are therefore two distinct types of quanidinate ligands in **4** in solution: terminal and bridging. The corresponding methyne *i*Pr resonances appear at 3.43, 3.65, 3.80, and 3.90 ppm.

Treatment of **4** with the Lewis bases THF and *tert*-butylisocyanide was performed in an attempt to disrupt the bridging guanidinate interaction. When samples of **4** dissolved in d_8-THF were analyzed by ^{1}H NMR spectroscopy at 20 °C, the spectrum was consistent with a monomeric adduct complex formulated as Sr(η^2-**2**L)$_2$(d_8-THF)$_n$ (**4′**, Scheme 2). The ^{1}H NMR spectrum of **4′** in d_8-THF only had resonances corresponding

Scheme 2

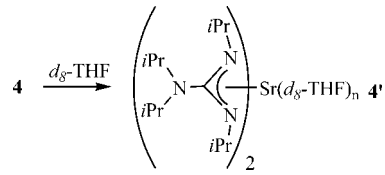

to one guanidinate ligand environment with two doublets for *i*Pr CH_3 groups at 0.98 and 1.15 ppm and two septets for *i*Pr methyne protons at 3.56 and 3.38 ppm. In separate experiments, samples of **4** were dissolved in THF, and the THF was then removed under reduced pressure. After THF removal, **4** was regenerated, as observed by ^{1}H NMR spectroscopy (in C_6D_6), and no adducted species remained in the mixture, even in the presence of residual THF. Samples of **4** in C_6D_6 were treated with up to 6.0 equiv of *tert*-butyl isocyanide at 20 °C. When the samples were analyzed by ^{1}H NMR spectroscopy, only resonances for **4** and free *tert*-butyl isocyanide were observed, indicating that *tert*-butyl isocyanide was not effective at disrupting the bridging guanidinate interaction in **4**.

In order to explore the possibility of isolating mixed-ligand guanidinate complexes, we focused on Cp* as an ancillary ligand and explored reactions of Sr(Cp*)$_2$[7c] with **1**LH and **2**LH. Treatment of Sr(Cp*)$_2$ with 1.0 equiv of **1**LH or **2**LH at 20 °C gave the mixed-ligand dimers **5** and **6**, respectively (Scheme 1). Crystals of **5** and **6** formed overnight from the reaction mixtures and were isolated by filtration. The ^{1}H and ^{13}C NMR spectra of **5** and **6** alone do not contain enough data to differentiate between monomeric or higher order structures. For example, the ^{1}H NMR spectrum of **6** shows resonances for one guanidinate ligand and one Cp* ligand. The guanidinate *i*Pr

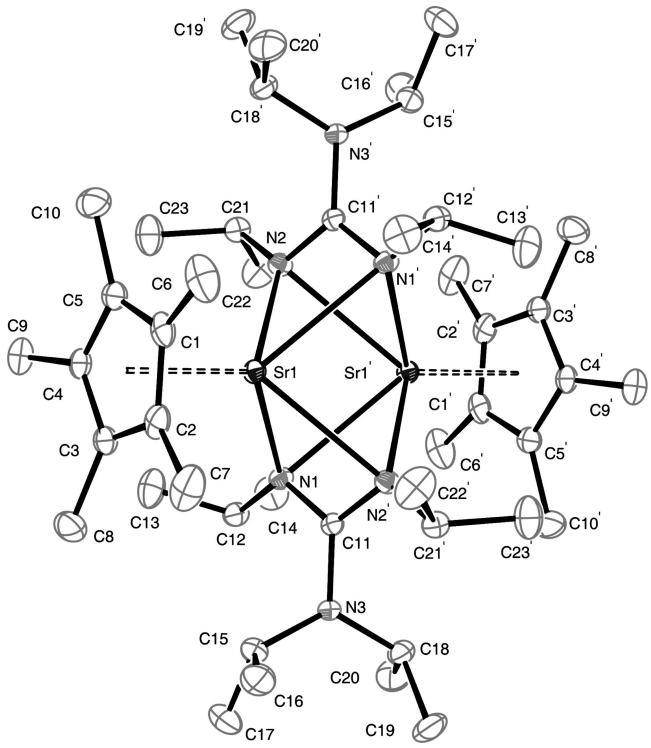

Figure 3. Thermal ellipsoid plot of **6** (30% probability thermal ellipsoids). Selected bond lengths (Å) and angles (deg): Sr(1)–N(1) 2.6371(18), Sr(1)–N(2) 2.6307(18), Sr(1)–N(1)′ 2.8269(19), Sr(1)–N(2)′ 2.8506(18), Sr(1)–Cp*(cent) 2.616(2), Sr(1)–Sr(1)′ 3.4769(5), Cp*(cent)–Sr(1)–N(1) 125.6(1), Cp*(cent)–Sr(1)–N(1′) 133.2(1), Cp*(cent)–Sr(1)–N(2) 124.6(1), Cp*(cent)–Sr(1)–N(2′) 133.9(1), N(2)′–C(11)–N(1) 114.04(18), N(1)′–Sr(1)–N(2) 48.56(5), N(1)–Sr(1)–N(2)′ 48.25(5).

methyl resonances appear as doublets at 1.21 and 1.31 ppm, the methyne septets have chemical shifts of 3.40 and 3.70 ppm, and the Cp* methyl groups appear at 2.11 ppm. On the basis of the above ^{1}H NMR data, **6** could be formulated as a monomer or a dimer. A single-crystal X-ray study was undertaken on a crystal of **6** to gain an understanding of the bonding in the compound. The details of the structure refinement appear in Table 1. The thermal ellipsoid plot of **6** is shown in Figure 3 and confirms the identity of **6** as a mixed-ligand dimer. In **6** the two strontium metal centers are best described as five-coordinate and are bridged by two $\mu^2,\eta^2{:}\eta^2$-guanidinate ligands. The τ value for Sr(1) in **6** is 0.55 (using Cp*(cent)-based angles), and the geometry is best described as nearly at a midpoint between trigonal bipyramidal and square pyramidal. The bite angles of the bridging ligands N(1)′−Sr(1)−N(2) and N(1)−Sr(1)−N(2)′ are 48.56(5)° and 48.25(5)°, respectively, and are comparable to the bite angles of the $\mu^2,\eta^2{:}\eta^2$-guanidinate ligands in **3** and **4**. The metal−guanidinate bond distances for Sr(1)−N(1), Sr(1)−N(2), Sr(1)−N(1)′, and Sr(1)−N(2)′ are 2.6371(18), 2.6307(18), 2.8269(19), and 2.8506(18) Å, respectively. The longest of the bond lengths are within the sum of the ionic radius of Sr^{2+} and the van der Waals radius of nitrogen (2.87 Å) and are thus considered bonding interactions.[14] The Sr(1)−Cp*(cent) distance of 2.616(2) Å is normal and, for example, compares well with the reported distance for Sr−Cp(cent) in $[(Cp^{3Si})Sr(\mu\text{-}I)(THF)_2]_2$ of 2.604(7) Å (Cp^{3Si} = 1,2,4-tris(trimethylsilyl)cyclopentadienyl).[9b] As mentioned above, this is a rare example of a crystallographically characterized, non-halide-containing, mixed-ligand Cp* strontium complex and the first reported example of a mixed-ligand, Cp*-guanidinate strontium complex.

Scheme 3

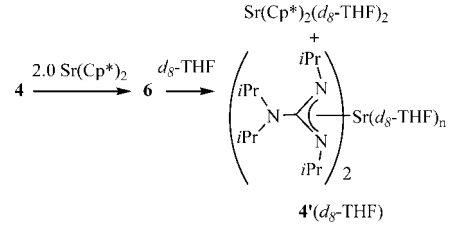

Table 2. Summary of Crystallographic Data and Structure Refinement Details for 7, 8, and 10

	7	**8**	**10**
empirical formula	$C_{52}H_{112}Ba_2N_{12}$	$C_{52}H_{92}Ba_2N_6$	$C_{30}H_{74}N_6OSi_4Sr$
fw	1180.22	1076.00	734.93
space group	*Pnnn*	*C*2*c*	*C*2/*c*
a (Å)	10.4350(8)	14.292(3)	29.443(2)
b (Å)	14.5080(11)	19.633(4)	9.6770(7)
c (Å)	19.9570(14)	19.719(4)	16.5960(12)
β (deg)	90	101.181(3)	110.4550(10)
V_c (Å^3)	3021.3(4)	5428.0(19)	4430.4(5)
D_c (Mg m^{-3})	1.297	1.317	1.102
Z	2	4	4
μ(Mo Kα) (mm^{-1})	1.337	1.479	1.353
final *R* indices[a]	R1 = 0.0362 wR2 = 0.0754 [3559]	R1 = 0.0899 wR2 = 0.2457 [6235]	R1 = 0.0261 wR2 = 0.0642 [5075]

[a] $R1 = \sum F_o| - |F_c/\sigma|F_o| \sum|F_o|$ and $wR2 = [\sum[w(F_o^2 - F_c^2)^2]/\sum[w(F_o^2)^2]]^{1/2}$. The parameter $w = 1/[\sigma^2(F_o^2) + (aP)^2]$.

When samples of **6** were placed in C_6D_6 and heated to 70 °C in sealed NMR tubes for days, no change in sample composition was observed by ^{1}H NMR spectroscopy or by visual inspection. However, when samples of **6** were gently heated in d_8-THF to promote dissolution, ligand redistribution to afford the parent homoleptic complexes $Sr(\eta^2\text{-}\mathbf{2}L)_2(d_8\text{-THF})_n$ (**4′**, d_8-THF) and $Sr(Cp^*)_2(d_8\text{-THF})_2$ was observed by ^{1}H NMR spectroscopy (Scheme 3). Samples of $Sr(Cp^*)_2$ and **4** were mixed in C_6D_6 and monitored by ^{1}H NMR spectroscopy to explore this Schlenk equilibrium. When **4** was treated with 2.0 equiv of $Sr(Cp^*)_2$ in C_6D_6, small amounts of **6** started to form within minutes, as observed by ^{1}H NMR spectroscopy at 20 °C (Scheme 3). When the sample was warmed to 60 °C, to increase the rate of reaction, conversion to **6** was almost complete after 40 min. As **6** formed in the NMR tube at 60 °C, it also crystallized from solution, making it difficult to measure the relative rate of conversion. The above ligand redistribution reactions are interesting, as they show that the mixed-ligand complex (**6**) is the favored complex as long as a Lewis base is not present in the mixture. This observation is different than the data presented for the group II mixed-ligand Cp-halides.[9] In the case of the Cp-halides, THF was shown to stabilize or favor the mixed-ligand complexes, and loss of THF led to homoleptic complexes. As mentioned, in our case, addition of THF to **6** gives the homoleptic THF adducts.

Similar reactivity trends were also observed for barium complexes. Treatment of $[Ba\{N(SiMe_3)_2\}_2(THF)_{1.6}]$ with 2.0 equiv of **2**LH at 20 °C gave dimeric **7**, the barium analogue to **4**, whereas reaction of $Ba(Cp^*)_2(THF)_{1.7}$ with **2**LH at 20 °C gave dimeric **8**, the barium analogue to **6** (Scheme 1). Single-crystal X-ray diffraction studies were carried out on crystals of **7** and **8**, and the details of the structure refinement appear in Table 2 (although single crystals of **8** were harvested for the crystallographic study, pure samples of **8** could not be prepared; see below). Each metal center in **7** is six-coordinate and supported by η^2-terminal and $\mu^2,\eta^2{:}\eta^2$-bridging ligands (Figure

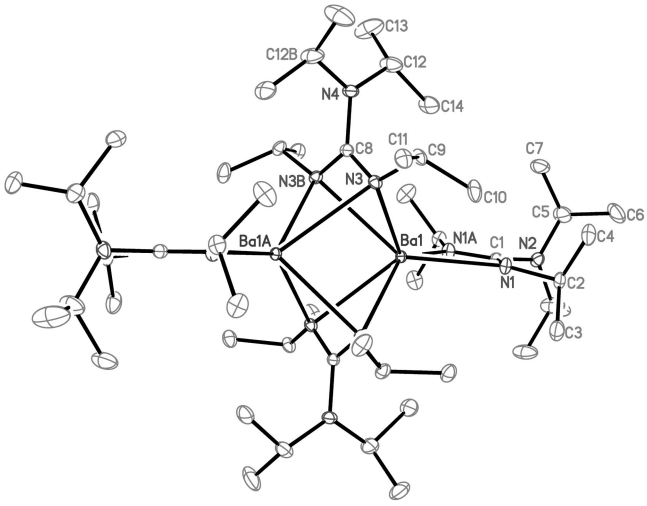

Figure 4. Thermal ellipsoid plot of **7** (30% probability thermal ellipsoids). Selected bond lengths (Å) and angles (deg): Ba(1)–N(1) 2.735(2), Ba(1)–N(1A) 2.735(2), Ba(1)–N(3) 2.830(2), Ba(1)–N(3B) 2.918(2), Ba(1)–Ba(1A) 3.7959(5), N(1)–Ba(1)–N(1A) 49.42(10), N(3)–Ba(1)–N(3B) 46.19(9), Ba(1)–Ba(1A) 3.7959(5).

4). The Ba(1)−N(1) and Ba(1)−N(1A) η^2-terminal metal distance of 2.735(2) Å is within the expected range, as it correlates well with the related average η^2-terminal metal distance in **3** of 2.566(2) Å, once the ionic radius difference of approximately 0.17 Å between strontium and barium is considered.[14] For comparison, the related $[PhC(NSiMe_3)_2]_2Ba(DME)(THF)$ has Ba−N amidinate interactions of 2.73 and 2.82 Å, where the slightly longer Ba−N amidinate bond can be attributed to the increased coordination number when compared to **7**. The Ba(1)−N(3) and Ba(1)−N(3B) distances of 2.830(2) and 2.918(2) Å, respectively, fall within the expected range for a $\mu^2,\eta^2:\eta^2$-bridging ligand when compared to **3**, **4**, and **6** once the difference in ionic radius between the different metals is considered.

Complex **8** crystallized from benzene in a monoclinic unit cell, and the thermal ellipsoid plot of **8** is shown in Figure 5 with selected bond lengths and angles. Compound **8** is best described as a five-coordinate, mixed-ligand dimer containing teminal Cp* ligands and $\mu^2,\eta^2:\eta^2$-bridging guanidinate ligands. The geometry about the metal centers in **6** and **8** is very similar, as the almost identical values for τ between the two compounds indicate ($\tau = 0.54$, Ba(1) **8**; $\tau = 0.55$, Sr(1) **6**). From a general point of view, all interactions in **8** are similar to those in **6** and only vary as a result of the differing ionic radii of strontium and barium. The Cp*(cent)−Ba(1) distance of 2.752(10) Å is comparable to the reported Cp(cent) distances in related monoring complexes such as $\{[(Cp^{3Si})BaI(THF)_2]\cdot 1/2C_7H_8\}_\infty$, 2.76(1) Å,[9b] and $[(C_5H_2(CMe_3)_3\text{-}1,2,4)Ba(\mu\text{-}I)(THF)_2]_\infty$, 2.762 Å.[9a]

Unfortunately we were not able to isolate **8** in pure form. Samples of **8** formed by crystallization from the reaction mixture, or by removal of solvent from the reaction mixture, always contained significant amounts of $Ba(Cp^*)_2(THF)_{1.7}$. When a sample of crystals, grown by slow evaporation of the reaction mixture at 20 °C, was isolated and analyzed by ^1H NMR spectroscopy in C_6D_6 at 60 °C, the ratio of $Ba(Cp^*)_2(THF)_{1.7}$ to **8** was 4:3.[16] The NMR sample was warmed to 60 °C to ensure that all material was dissolved during the NMR spectroscopy experiment. We propose that a Schlenk equilibrium, similar to that discussed above for **6** (Scheme 3), could explain this result. We have not made any additional attempts at isolating pure samples of **8**.

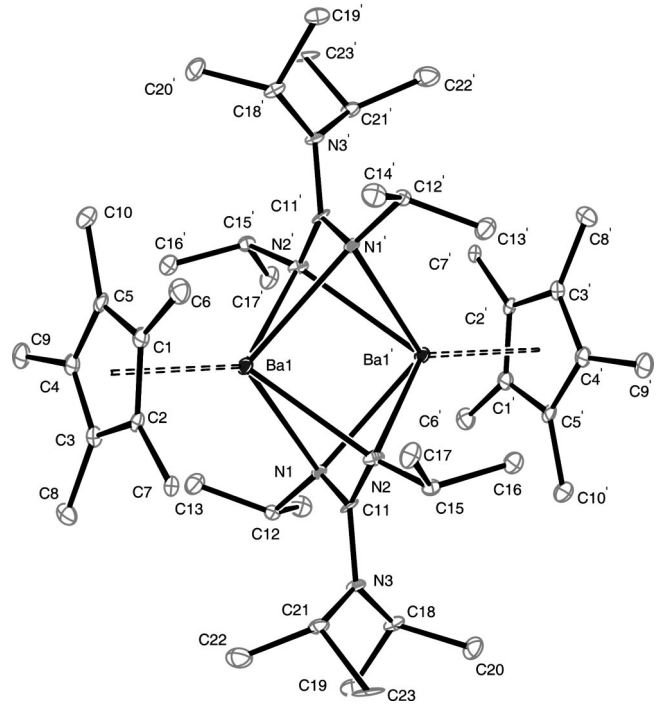

Figure 5. Thermal ellipsoid plot of **8** (30% probability thermal ellipsoids). Selected bond lengths (Å) and angles (deg): Ba(1)–N(1) 2.972(8), Ba(1)–N(2) 2.769(9), Ba(1)–N(1′) 2.819(9), Ba(1)–N(2′) 2.877(9), Ba(1)–Cp*(cent) 2.752(10), N(1)–C(11)–N(2) 114.7(9), N(1)–Ba(1)–N(2)46.3(2),N(1′)–Ba(1)–N(2′)46.8(2),Cp*(cent)–Ba(1)–N(1) 133.4(3), Cp*(cent)–Ba(1)–N(1′) 125.3(3), Cp*(cent)–Ba(1)–N(2) 127.6(3), Cp*(cent)–Ba(1)–N(2′) 133.5(3).

Scheme 4

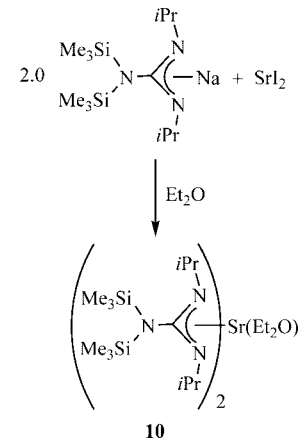

10

In an effort to generate monomeric strontium complexes, the reaction between SrI_2 and $Na[(iPr)NC(N(SiMe_3)_2)N(iPr)]$ in diethyl ether was performed (Scheme 4). After stirring for 8 days at 20 °C, the mixture was filtered, and the solvent was removed from the filtrate to afford **10** as a white solid. A single-crystal X-ray study was undertaken on a crystal of **10** grown from a pentane solution at −30 °C. The monomeric, five-coordinate nature of **10** is confirmed by the thermal ellipsoid plot shown in Figure 6. The geometry about the metal in **10** can be best described in a fashion similar to the related five-coordinate structures **3**, **6**, and **8** and has a τ value of 0.62. The η^2-terminal ligands in **10** are twisted with respect to one another and show bonding parameters similar to those already discussed in **3** and **4**. For comparative purposes, the important bond lengths and angles for **10** are summarized in Figure 6. We propose that the monomeric nature of **10**, when compared to **3** and **4**, is a

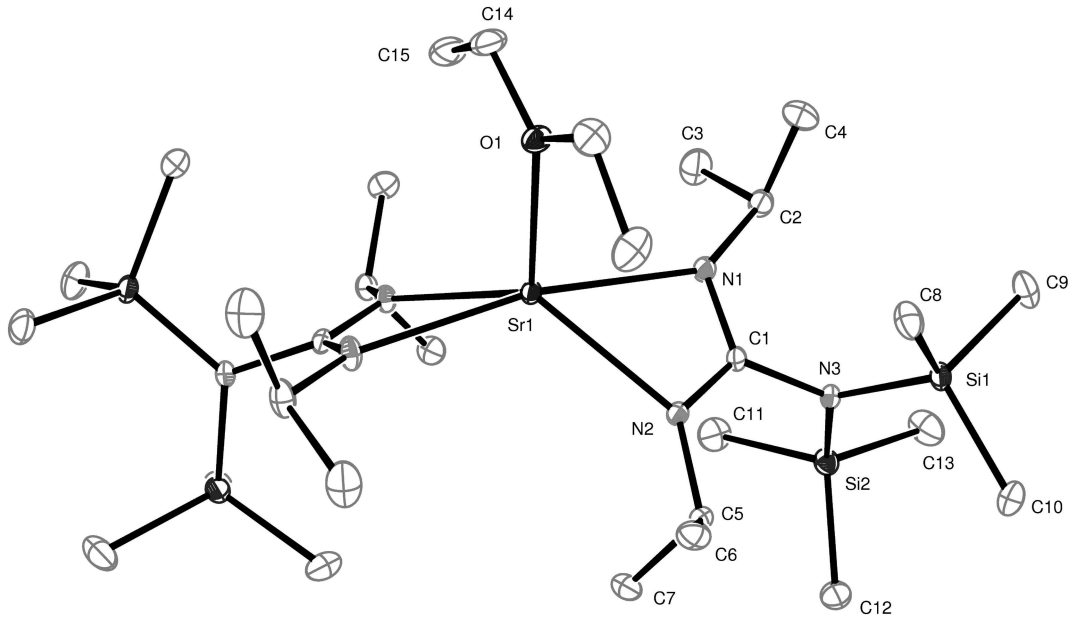

Figure 6. Thermal ellipsoid plot of **10** (30% probability thermal ellipsoids). Selected bond lengths (Å) and angles (deg): Sr(1)–O(1) 2.5246(14), Sr(1)–N(1) 2.5603(11), Sr(1)–N(2) 2.5136(11), C(1)–N(3) 1.4605(16), N(1)–C(1)–N(2) 116.88(11), N(1)–Sr(1)–N(2) 52.86(4).

result of the larger steric requirement of the $SiMe_3$ group. Complex **10** is an analogue to the above-mentioned [Sr{(Cy)-NC(N($SiMe_3$)$_2$)N(Cy)}$_2$·(Et_2O)], five-coordinate, C_2-symmetric complex reported by Harder et al.[2c] The average Sr−N bond length in **10** is 2.5370(11) Å and is similar to the average Sr−N bond length of 2.524(3) Å in [Sr{(Cy)NC(N($SiMe_3$)$_2$)N-(Cy)}$_2$·(Et_2O)]. In addition to [Sr{(Cy)NC(N($SiMe_3$)$_2$)-N(Cy)}$_2$·(Et_2O)], the class of compound represented by **10** is related to recently published monomeric and homoleptic lanthanide(II) bis(guanidinate) complexes.[17] For comparative purposes, the average Sr−N bond length in **10** of 2.5370(11) Å is very similar to the average M−N distances of 2.546(2) and 2.540(2) Å in [Sm{(ArN)$_2$CN(C_6H_{11})$_2$}$_2$] and [Eu{(ArN)$_2$ CN(C_6H_{11})$_2$}$_2$], respectively (Ar = (C_6H_3)*i*Pr$_2$-2,6).[17a] This is, of course, as expected since the ionic radii of Sr^{2+} (1.32 Å), Sm^{2+} (1.36 Å), and Eu^{2+} (1.31 Å) do not differ to a great extent.[18]

Experimental Section

General Methods. Compounds [Sr{N($SiMe_3$)$_2$}$_2$]$_2$ and [Ba{N ($SiMe_3$)$_2$}$_2$(THF)$_{1.6}$] were prepared by a modified literature procedure as outlined in the experimental section.[19] Compounds Sr(Cp*)$_2$ and Ba(Cp*)$_2$(THF)$_{1.7}$ were synthesized according to a literature procedure with the variation that coordinated Et_2O was removed from Sr(Cp*)$_2$(Et_2O) by sublimation and not by the reported toluene reflux procedure.[7c] All starting materials were purchased from Aldrich. KN($SiMe_3$)$_2$ was prepared by treating HN($SiMe_3$)$_2$ with KH. All reactions were conducted under a dry nitrogen atmosphere using standard Schlenk techniques or in a nitrogen-filled drybox. All solvents were distilled under inert gas from sodium or sodium benzophenone ketyl or passed over activated alumina, stored over molecular sieves, and degassed prior to use. All NMR spectra were obtained on a Varian Mercury 300 instrument with C_6D_6, d_8-toluene, or d_8-THF as solvents and referenced to residual solvent peaks. Elemental analyses were performed by CALI Laboratories, Parsippany, NJ. In the case of **5** the results obtained were not satisfactory. Difficulties in characterizing metal compounds by elemental analysis have also been encountered by other researchers.[20] We have included a ^{1}H NMR spectrum of **5** in the Supporting Information to show the purity of **5** by ^{1}H NMR spectroscopy.

Crystallography (for 3, 4, 6, 7, 8, and 10). All data were integrated using the Bruker SAINT software program[21] and scaled using the SADABS software program.[22] Solution by direct methods (SIR-2004) produced a complete heavy-atom phasing model consistent with the proposed structure. All non-hydrogen atoms were refined anisotropically by full-matrix least-squares (SHELXL-97).[23] All hydrogen atoms were placed using a riding model. Their positions were constrained relative to their parent atom using the appropriate HFIX command in SHELXL-97.

Synthesis of [Sr{N($SiMe_3$)$_2$}$_2$]$_2$. To a stirring SrI_2 (7.00 g, 20.50 mmol) diethyl ether suspension (175 mL) was added KN($SiMe_3$)$_2$ (8.16 g, 41.00 mmol). After 2 days of stirring at 20 °C, the reaction mixture was filtered with a 0.2 μm filter, and the filtrate was concentrated under reduced pressure, giving 5.95 g of [Sr{N ($SiMe_3$)$_2$}$_2$]$_2$, yield = 71%. ^{1}H NMR (d_8-toluene, 20 °C): δ 0.24. ^{13}C{^{1}H} NMR (d_8-toluene, −63 °C): δ 6.2, 6.3.

Synthesis of [Ba{N($SiMe_3$)$_2$}$_2$(THF)$_{1.6}$]. To a stirring BaI_2 (1.08 g, 2.77 mmol) THF suspension (30 mL) was added KN($SiMe_3$)$_2$ (1.10 g, 5.53 mmol). After 3.5 days of stirring at 20 °C, the THF was removed under reduced pressure. The remaining white solid was triturated twice with 20 mL of pentane. The white solid was then extracted with 2 × 30 mL of pentane and filtered through a 0.2 μm filter, and the filtrate was concentrated under reduced pressure giving 0.99 g of [Ba{N($SiMe_3$)$_2$}$_2$(THF)$_{1.6}$], yield = 60%. ^{1}H NMR (C_6D_6, 20 °C): δ 0.31 (36H, Si*Me*$_3$), 1.29 (mult, THF C*H*$_2$), 3.45 (mult, THF OC*H*$_2$).

(17) (a) Heitmann, D.; Jones, C.; Junk, P. C.; Lippert, K.; Stasch, A. *Dalton Trans.* **2007**, 187. (b) Cole, M. L.; Junk, P.C. *Chem. Commun.* **2005**, 2695. (c) Wedler, M.; Noltemeyer, M.; Pieper, U.; Schmidt, H.-G.; Stalke, D.; Edelmann, F. T. *Angew. Chem., Int. Ed. Engl.* **1990**, *29*, 894.

(18) Radii taken from: Huheey, J. E. *Inorganic Chemisty*, 3rd ed.; Harper & Row: New York, 1983.

(19) Brady, E. D.; Hanusa, T. P.; Pink, M.; Young, V. G., Jr. *Inorg. Chem.* **2000**, *39*, 6028.

(20) (a) Arndt, S.; Voth, P.; Spaniol, T. P.; Okuda, J. *Organometallics* **2000**, *19*, 4690. (b) Mitchell, J. P.; Hajela, S.; Brookhart, S. K.; Hardcastle, K. I.; Henling, L. M.; Bercaw, J. E. *J. Am. Chem. Soc.* **1996**, *118*, 1045.

(21) *SAINT-NT* 5.050; Bruker AXS, Inc.: Madison, WI, 1998.

(22) Sheldrick, G. *SADABS*, first release; University of Göttingen: Germany.

(23) *SHELXTL NT*, Version 5.10; Bruker AXS, Inc.: Madison, WI, 1997.

Synthesis of Lithium Diisopropylamide (LDA). To a stirring solution of diisopropylamine in pentane (10.0 g, 98.8 mmol, 13.96 mL, 200 mL of pentane) was added butyllithium (61.75 mL, 98.8 mmol, 1.6 M in hexane) at 0 °C. The reaction was warmed to 20 °C and stirred for an additional 3 h. The pentane was removed under reduced pressure to afford LDA as a white solid. The LDA was used without further purification.

Synthesis of *i*PrN═C(NMe$_2$)N(H)*i*Pr (1LH). To a stirring solution of diisopropylcarbodiimide (10.0 g, 79.2 mmol, 125 mL of ether) was added solid LiNMe$_2$ (4.04 g, 79.2 mmol, Aldrich). The reaction was stirred overnight at 20 °C, filtered, and concentrated under reduced pressure to give a yellow oil that solidified over time and was identified as Li(*i*PrNC(NMe$_2$)N*i*Pr) by ^{1}H NMR spectroscopy. ^{1}H NMR (C$_6$D$_6$, 20 °C): δ 1.25 (br, *i*Pr, *Me*), 2.63 (br, N*Me*$_2$), 3.75 (br, *i*Pr, C*H*); residual Et$_2$O was observed by ^{1}H NMR spectroscopy in the crude product. To a stirring solution of Li(*i*PrNC(NMe$_2$)N*i*Pr) (10.66 g, 60.0 mmol, 175 mL of toluene) was added excess water (20 mL). The mixture was stirred for 30 min. The toluene was then separated from the water layer, and the water layer was extracted twice with 50 mL of toluene. The toluene layer was dried over molecular sieves and concentrated using a rotary evaporator to give 7.0 g of crude *i*PrN═C(NMe$_2$)N(H)*i*Pr, as confirmed by ^{1}H NMR spectroscopy. The crude oil was distilled under reduced pressure to give pure *i*PrN(H)C(NMe$_2$)═N*i*Pr. ^{1}H NMR (C$_6$D$_6$, 20 °C): δ 0.86 (d, $^3J_{HH}$ = 6.5 Hz, 6H, *i*Pr *Me*), 1.24 (d, $^3J_{HH}$ = 6.0 Hz, 6H, *i*Pr *Me*), 2.63 (6H, N*Me*$_2$), 2.95 (br, N*H*), 3.28 (mult, 2H, *i*Pr C*H*).

Synthesis of *i*PrN═C(N(*i*Pr)$_2$)N(H)*i*Pr (2LH). To a stirring solution of diisopropylcarbodiimide (10.0 g, 79.2 mmol, 125 mL of ether) was added freshly prepared solid LDA (8.48 g, 79.2 mmol). During the LDA addition the reaction warmed slightly. After 4 h of stirring at 20 °C, a white precipitate formed in the reaction flask, and the ether was removed under reduced pressure. The white solid was then triturated with 30 mL of pentane, dried under reduced pressure, and identified as an ether adduct of Li(*i*PrNC(N(*i*Pr)$_2$)N*i*Pr) by ^{1}H NMR spectroscopy. ^{1}H NMR (C$_6$D$_6$, 20 °C): δ 1.11 (t, $^3J_{HH}$ = 7.0 Hz, 6H, Et$_2$O, *Me*), 1.23 (br, d, $^3J_{HH}$ = 6.5 Hz, 12H, *i*Pr *Me*), 1.30 (br, d, $^3J_{HH}$ = 6.0 Hz, 12H, *i*Pr *Me*), 3.25 (q, $^3J_{HH}$ = 7.0 Hz, 4H, Et$_2$O, C*H*$_2$), 3.48 (sept, $^3J_{HH}$ = 6.5 Hz, 2H, *i*Pr C*H*), 3.79 (sept, $^3J_{HH}$ = 6.0 Hz, 2H, *i*Pr C*H*). To a stirring solution of Li(*i*PrNC(N(*i*Pr)$_2$)N*i*Pr) (17.28 g, 74.0 mmol, 200 mL of toluene) was added excess water (26.6 mL). The mixture was stirred for 1 h. The toluene was then separated from the water layer, and the water layer was extracted twice with 50 mL of toluene. The toluene layer was dried over molecular sieves and concentrated using a rotary evaporator to give 13.7 g of crude *i*PrN═C(N(*i*Pr)$_2$)N(H)*i*Pr, as confirmed by ^{1}H NMR spectroscopy. It is important to note that this guanidine exists as a mixture of isomers in solution at 20 °C, as shown by ^{1}H NMR spectroscopy: the isomers were not identified; however, there is literature precedent for this behavior.[24] ^{1}H NMR (C$_6$D$_6$, 20 °C): δ 0.89 (d, $^3J_{HH}$ = 6.5 Hz, *i*Pr *Me*), 0.98 (d, $^3J_{HH}$ = 6.5 Hz, *i*Pr *Me*), 1.8 (br), 1.21 (d, $^3J_{HH}$ = 6.0 Hz, *i*Pr *Me*), 1.30 (d, $^3J_{HH}$ = 7.0 Hz, *i*Pr *Me*), 2.95 (ov, br, mult), 3.40 (ov, br, mult), 3.60 (sept, $^3J_{HH}$ = 7.0 Hz, *i*Pr C*H*), 4.18 (br). MS: *m/e* 184.

Synthesis of [(η^2-1L)Sr(μ^2,η^2:η^2-1L)(μ^2,η^1:η^1-1L)Sr(η^2-1L)] (3). To a toluene or benzene solution of [Sr{N(SiMe$_3$)$_2$}$_2$]$_2$ (0.31 g, 0.38 mmol, 10 mL of solvent) was added 4.0 equiv of *i*PrN═C(NMe$_2$)N(H)*i*Pr (**1**LH) (0.26 g, 1.50 mmol) at 20 °C. On standing, X-ray quality crystals of **3** formed overnight and were isolated by filtration in 69% yield. ^{1}H NMR (C$_6$D$_6$, 60 °C):[16] δ 1.24 (d, $^3J_{HH}$ = 6.5 Hz, 24H, *i*Pr *Me*), 1.40 (d, $^3J_{HH}$ = 6.5 Hz, 24H, *i*Pr *Me*), 2.71 (12H, N*Me*), 2.77 (12H, N*Me*), 3.65 (mult, ov, 8H, *i*PrC*H*). ^{13}C{^{1}H} NMR (C$_6$D$_6$, 60 °C):[16] δ 27.0, 28.3, 41.7, 41.9, 46.9, 47.7, 169.9, 170.7. Anal. Calcd for C$_{36}$H$_{80}$N$_{12}$Sr$_2$: C, 50.51; H, 9.35; N, 19.64. Found: C, 50.34; H, 9.48; N, 19.49.

Synthesis of [(η^2-2L)Sr(μ^2,η^2:η^2-2L)$_2$Sr(η^2-2L)] (4). To a toluene or benzene solution of [Sr{N(SiMe$_3$)$_2$}$_2$]$_2$ (0.60 g, 0.74 mmol, 10 mL of solvent) was added 4.0 equiv of *i*PrN═C(N(*i*Pr)$_2$)N(H)*i*Pr (**2**LH) (0.66 g, 2.96 mmol) at 20 °C. On standing, X-ray quality crystals of **4** formed overnight and were isolated by filtration in 72% yield. ^{1}H NMR (C$_6$D$_6$, 60 °C):[16] δ 1.20 (d, $^3J_{HH}$ = 6.5 Hz, 24H, *i*Pr *Me*), 1.23 (d, $^3J_{HH}$ = 6.0 Hz, 24H, *i*Pr *Me*), 1.30 (d, $^3J_{HH}$ = 7.0 Hz, 24H, *i*Pr *Me*), 1.48 (d, $^3J_{HH}$ = 6.5 Hz, 24H, *i*Pr *Me*), 3.43 (sept, $^3J_{HH}$ = 6.5 Hz, 4H, *i*Pr C*H*), 3.65 (sept, $^3J_{HH}$ = 7.0 Hz, 4H, *i*Pr C*H*), 3.80 (sept, $^3J_{HH}$ = 6.0 Hz, 4H, *i*Pr C*H*), 3.90 (sept, $^3J_{HH}$ = 6.5 Hz, 4H, *i*Pr C*H*). ^{13}C {^{1}H} NMR (C$_6$D$_6$, 60 °C):[16] δ 23.5, 25.0, 28.0, 28.1, 47.1, 48.1, 48.3, 51.4, 167.5, 172.4. Anal. Calcd for C$_{52}$H$_{112}$N$_{12}$Sr$_2$: C, 57.82; H, 10.38; N, 15.57. Found: C, 57.74; H, 10.45; N, 15.40.

Synthesis of [(Cp*)Sr(μ^2,η^2:η^2-1L)$_2$Sr(Cp*)] (5). To a benzene solution of Sr(Cp*)$_2$ (0.20 g, 0.56 mmol, 15 mL of solvent) was added *i*PrN═C(NMe$_2$)N(H)*i*Pr (**1**LH) (0.095 g, 0.56 mmol) at 20 °C. On standing at 20 °C, X-ray quality crystals of **5** formed and were isolated by filtration in 68% yield. ^{1}H NMR (C$_6$D$_6$, 60 °C):[16] δ 1.14 (d, $^3J_{HH}$ = 6.5 Hz, 24H, *i*Pr *Me*), 2.12 (30H, Cp* *Me*), 2.61 (12H, N*Me*), 3.38 (sept, $^3J_{HH}$ = 6.5 Hz, 4H, *i*Pr C*H*). ^{13}C {^{1}H} NMR (C$_6$D$_6$, 60 °C):[16] δ 12.3, 26.9, 41.8, 47.3, 113.7, 170.9. Anal. Calcd for C$_{38}$H$_{70}$N$_6$Sr$_2$: C, 58.07; H, 8.91; N, 10.70. Found: C, 54.44; H, 8.86; N, 10.00.

Synthesis of [(Cp*)Sr(μ^2,η^2:η^2-2L)$_2$Sr(Cp*)] (6). To a benzene solution of Sr(Cp*)$_2$ (0.10 g, 0.28 mmol, 8.0 mL of solvent) was added *i*PrN═C(N(*i*Pr)$_2$)N(H)*i*Pr (**2**LH) (0.063 g, 0.28 mmol) at 20 °C. On standing at 20 °C, X-ray quality crystals of **6** formed and were isolated by filtration in 80% yield. ^{1}H NMR (C$_6$D$_6$, 60 °C):[16] δ 1.21 (d, $^3J_{HH}$ = 6.5 Hz, 24H, *i*Pr *Me*), 1.31 (d, $^3J_{HH}$ = 7.0 Hz, 24H, *i*Pr *Me*), 2.11 (30H, Cp* *Me*), 3.40 (sept, $^3J_{HH}$ = 7.0 Hz, 4H, *i*Pr C*H*), 3.70 (sept, $^3J_{HH}$ = 6.5 Hz, 4H, *i*Pr C*H*). ^{13}C{^{1}H} NMR (C$_6$D$_6$, 60 °C):[16] δ 12.5, 25.3, 27.0, 47.6, 52.1, 114.1, 173.0. Anal. Calcd for C$_{46}$H$_{86}$N$_6$Sr$_2$: C, 61.52; H, 9.58; N, 9.36. Found: C, 61.29; H, 9.68; N, 9.16.

Synthesis of [(η^2-2L)Ba(μ^2,η^2:η^2-2L)$_2$Ba(η^2-2L)] (7). To a benzene solution of [Ba{N(SiMe$_3$)$_2$}$_2$(THF)$_{1.6}$] (0.21 g, 0.35 mmol, 4 mL of solvent) was added 2.1 equiv of *i*PrN═C(N(*i*Pr)$_2$)N(H)*i*Pr (**2**LH) (0.17 g, 0.73 mmol) at 20 °C. On standing, X-ray quality crystals of **7** formed overnight and were isolated by filtration in 83% yield. ^{1}H NMR (C$_6$D$_6$, 60 °C):[16] δ 1.19 (d, $^3J_{HH}$ = 6.5 Hz, 24H, *i*Pr *Me*), 1.20 (d, $^3J_{HH}$ = 6.5 Hz, 24H, *i*Pr *Me*), 1.23 (d, $^3J_{HH}$ = 6.5 Hz, 24H, *i*Pr *Me*), 1.49 (d, $^3J_{HH}$ = 6.5 Hz, 24H, *i*Pr *Me*), 3.43 (ov, mult, 8H, *i*Pr C*H*), 3.82 (sept, $^3J_{HH}$ = 6.5 Hz, 4H, *i*Pr C*H*), 3.93 (sept, $^3J_{HH}$ = 6.5 Hz, 4H, *i*Pr C*H*). ^{13}C{^{1}H} NMR (C$_6$D$_6$, 60 °C):[16] δ 23.6, 24.2, 28.1, 28.3, 47.2, 48.3, 48.4, 49.7, 166.2, 166.3. Anal. Calcd for Ba$_2$C$_{52}$H$_{112}$N$_{12}$: C, 52.94; H, 9.50; N, 14.25. Found: C, 52.02; H, 9.37; N, 13.99.

Synthesis of [(Cp*)Ba(μ^2,η^2:η^2-2L)$_2$Ba(Cp*)] (8). To a benzene solution of Ba(Cp*)$_2$(THF)$_{1.7}$ (0.25 g, 0.45 mmol, 10 mL of solvent) was added *i*PrN═C(N(*i*Pr)$_2$)N(H)*i*Pr (**2**LH) (0.10 g, 0.45 mmol) at 20 °C. On standing at 20 °C, X-ray quality crystals of **8** formed and were isolated by filtration. As mentioned in the discussion section, pure samples of **8** could not be prepared, and samples of **8** always contained Ba(Cp*)$_2$(THF)$_{1.7}$, as determined by ^{1}H NMR spectroscopy. Only ^{1}H NMR spectroscopic data were collected in addition to the single-crystal X-ray study on **8**. ^{1}H NMR (C$_6$D$_6$, 60 °C):[16] δ 1.21 (d, $^3J_{HH}$ = 6.0 Hz, 24H, *i*Pr *Me*), 1.24 (d, $^3J_{HH}$ = 7.0 Hz, 24H, *i*Pr *Me*), 2.11 (30H, Cp* *Me*), 3.25 (sept, $^3J_{HH}$ = 7.0 Hz, 4H, *i*Pr C*H*), 3.76 (sept, $^3J_{HH}$ = 6.0 Hz, 4H, *i*Pr C*H*).

Synthesis of [Sr(η^2-9L)$_2$OEt$_2$] (10). To a stirring 20 mL ether suspension of SrI$_2$ (1.00 g, 2.93 mmol) was added Na[(*i*Pr)-NC(N(SiMe$_3$)$_2$)N(*i*Pr)] (**9**LNa) (1.811 g, 5.85 mmol) at 20 °C. The mixture was stirred for 8 days and filtered through a 0.2

(24) (a) Schmidt, J. A. R.; Arnold, J. *Chem. Commun.* **1999**, 2149. (b) Coles, M. P. *Dalton Trans*. **2006**, 985.

μm filter. The resulting filtrate was concentrated under reduced pressure to afford 1.33 g of [Sr(η^2-**9**L)$_2$OEt$_2$] (**10**). ^{1}H NMR (C_6D_6, 20 °C): δ 0.36 (36H, N(Si*Me*$_3$)$_2$), 1.14 (t, 6H, ether, *Me*), 1.20 (d, 24H, *i*Pr *Me*), 3.2 (br, 4H, ether C*H*$_2$), 3.80 (br, sept, 4H, *i*Pr C*H*). ^{13}C{^{1}H} NMR (C_6D_6, 20 °C): δ 3.2, 15.7, 29.0, 46.7, 66.8, 163.6. Anal. Calcd for $SrC_{30}H_{74}N_6OSi_4$: C, 49.05; H, 10.08; N, 11.45. Found: C, 48.76; H, 9.81; N, 11.32. Single crystals of **10** were grown from a concentrated pentane solution at −30 °C.

Reaction of Sr(Cp*)$_2$ with [(η^2-2L)Sr(μ^2,η^2:η^2-2L)$_2$Sr(η^2-2L)] (4). To a C_6D_6 solution of Sr(Cp*)$_2$ (13 mg, 0.037 mmol, 0.4 mL of C_6D_6) was added **4** (20 mg, 0.019 mmol) in 0.4 mL of C_6D_6. The mixture was placed in an NMR tube and analyzed by ^{1}H NMR spectroscopy as described in the text.

Acknowledgment. We acknowledge ATMI for funding the research outlined herein and M. A. Petruska for valuable discussions.

Supporting Information Available: CIF files for **3**, **4**, **6**, **7**, **8**, and **10** and a ^{1}H NMR spectrum of **5**. This material is available free of charge via the Internet at http:/pubs.acs.org.

OM701118J